Astron. Astrophys. 340, 257–264 (1998)

ASTRONOMY AND ASTROPHYSICS

Deduced spectrum of interacting protons accelerated after the impulsive phase of the 15 June 1991 solar flare

L. Kocharov[1], H. Debrunner[2], G. Kovaltsov[1,⋆], J. Lockwood[3], M. McConnell[3], P. Nieminen[2], G. Rank[4], J. Ryan[3], and V. Schönfelder[4]

[1] Space Research Laboratory, University of Turku, Turku FIN-20014, Finland
[2] Physical Institute, University of Bern, CH-3012 Bern, Switzerland
[3] Space Science Center, University of New Hampshire, Durham NH 03824, USA
[4] Max Planck Institute for Extraterrestrial Physics, P.O. Box 1603, D-85740 Garching, Germany

Received 11 March 1998 / Accepted 15 September 1998

Abstract. In June 1991 the Sun produced a famous series of six powerful flares. For the solar eruption on 15 June 1991 there exists a rich set of measurements, including in particular γ-ray and neutron observations of the COMPTEL instrument on board the COMPTON Gamma Ray Observatory (CGRO) satellite. The γ-ray and neutron emissions indicate prolonged acceleration of protons well after the impulsive phase of the flare. Some accelerated particles interact with solar matter and produce γ-rays and neutrons at the Sun, others escape into the interplanetary medium. Here we present the deduced energy spectrum of the interacting protons for a nearly one hour period in the gradual phase of the flare. From the low-energy γ-ray and neutron results of COMPTEL we determine the energy spectrum of the interacting protons in the 10–200 MeV range. We find that the COMPTEL data are consistent with a proton power law spectrum with index 3.3 ± 0.1. To simultaneously fit the high-energy γ-ray measurements on board the GAMMA-1 satellite, the spectrum must steepen at a few hundred MeV and then become harder again to produce a detectable amount of GeV photons. Although the degree of steepening is composition dependent, the deduced spectrum of interacting protons is qualitatively invariant in the entire parameter region $\alpha/\mathrm{p} \leq 0.5$.

Key words: Sun: activity – Sun: flares – Sun: particle emission – Sun: X-rays, gamma rays

1. Introduction

The flare on 15 June 1991 (3B/X12, N33 W69) was one in a series of six X-class flares that all originated from the active region NOAA 6659 during its transit on the solar disk. These powerful events were extensively discussed in a number of publications (Ryan et al. 1993, Trottet et al. 1993, Kocharov et al. 1994, Ryan & McConnell 1995, Kane et al. 1995, Rank et al. 1995, Akimov et al. 1996, Lockwood et al. 1997, and references therein). However the neutron observations of the 15 June 1991 flare have not been completely analyzed. A fascinating property of this flare was a prolonged acceleration of high-energy protons responsible for γ-ray and neutron emissions generated during more than one hour after the impulsive phase (Kocharov et al. 1994). Akimov et al. (1996) suggested that acceleration of protons up to GeV energies may take place in a reconnecting current sheet forming behind a rising coronal mass ejection. On the other hand, shock waves also can accelerate solar particles (e.g., Kahler 1994). For the verification of an acceleration model, a knowledge of proton energy spectra is required.

To deduce spectra of high-energy ions interacting at the Sun, one should use γ-ray and neutron emissions (for a review see Mandzhavidze & Ramaty 1993). For instance, the 2.22 MeV to the 4–7 MeV γ-ray-line fluence ratio is a sensitive function of the ion spectrum slope at ~ 30 MeV, but it gives almost no information about the proton spectrum above 100 MeV. To deduce the energy spectrum of the interacting protons at higher energies, > 100 MeV, one has to employ the observed > 50 MeV neutrons and π^0-decay γ-rays. The COMPTEL instrument on board CGRO is sensitive to γ-rays in the energy range from 0.75 to 30 MeV (Schönfelder et al. 1993). COMPTEL can also image solar neutrons and measure the individual neutron energies in the energy range from approximately 10 MeV to 100 MeV (McConnell et al. 1993). Here we present a joint analysis of γ-rays and neutrons detected with COMPTEL on 15 June 1991. We also employ the high-energy γ-ray observations on board the GAMMA-1 satellite most recently analyzed by Djantemirov et al. (1995) and Chesnokov et al. (1995).

2. Neutron and γ-ray line emissions

Optical and radio observations indicate that the gradual phase of the 15 June 1991 flare started at about 8:26 UT (Fig. 1). The COMPTEL instrument was able to detect 10–100 MeV solar neutrons arriving at the Earth orbit during the period from $T_0^{\oplus}$ =09:02 UT to $T_1^{\oplus}$ =09:37 UT. The registered neutrons were produced at the Sun during the time interval corresponding to the electromagnetic-emission near-Earth arrival times from 8:12 to 9:25 UT. This includes both the impulsive and the grad-

⋆ *Present address:* A.F. Ioffe Physical-Technical Institute, St. Petersburg 194021, Russia

ual phase of the flare. However, due to the velocity dispersion, neutron monitoring time-intervals are energy dependent, so that only some portion of the flare was observed in a specified neutron energy channel. The start and end times of the energy dependent monitoring period can be denoted as $T_0(E)$ and $T_1(E)$. These times are shown in the upper panel of Fig. 1 along with the time-energy coordinates of the individual neutrons detected. To illustrate the relative timing of the neutron, γ-ray and microwave productions, the neutron time coordinates and the near-Earth times $T_0^{\oplus}$ and $T_1^{\oplus}$ have been shifted by the energy dependent difference between the Sun-Earth transit times for neutrons and electromagnetic radiation,

$$\Delta T(E) = \frac{R}{c}\Big[\frac{\gamma}{\sqrt{\gamma^2-1}} - 1\Big], \qquad (1)$$

where γ is the neutron Lorentz-factor, R =1 AU, and c is the speed of light. For instance, $T_0(E) = T_0^{\oplus} - \Delta T(E)$.

The energy dependent neutron monitoring periods and the limited statistics complicate the analysis and require some neutron production model to be adopted. The employed model of the neutron production during the flare is based on the multi-wavelength analyses carried out by Kocharov et al. (1994) and Akimov et al. (1996). In the frame of this model, the time profile of the neutron production is adopted to be similar to the profile of ~ 9 GHz microwave emission, $j_{mw}(t)$. We would like to stress that the microwave emission profile was selected because it fits the γ-ray profiles observed both by COMPTEL and GAMMA-1 (see Fig. 1). In fact, we primarily proposed the neutron injection profile to follow that for the γ-rays. Then, the microwave profile was used for approximating and extrapolating of the observed γ-ray profiles. We employ the 8.4 GHz emission intensity-time profile observed at Bern (Fig. 1, Andreas Magun, private communication 1995). This profile covers just the gradual phase of the flare. The impulsive phase was missed also by the γ-ray observations. For this reason, we prefer to drop the study of the impulsive phase in the present analysis. Neutrons produced during the impulsive phase, $\approx 12\%$ of the total number of neutrons registered by COMPTEL, are therefore excluded (these neutrons are seen in Fig. 1 to the left of the vertical line T_s =08:26 UT). All proton and neutron spectra which will be shown in present paper are normalized to the radio observation-period, 08:26–09:25 UT. The energy spectrum of the neutrons produced at the Sun is assumed to remain constant throughout the period, because available experimental data seem to be insufficient for studying a spectral evolution inside the gradual phase of the flare.

We calculate the numbers of neutrons in four selected energy channels, 10.0–18.4, 18.4–30.0, 30.0–52.0, and 52.0–100.0 MeV. For the energy channel from E_i to E_{i+1}, the number of observed neutron counts is given by

$$N_i = \frac{1}{R^2}\int_{E_i}^{E_{i+1}} \frac{f(E)}{W(T_0^*(E), T_1(E))} A(E)P(E)\mathrm{d}E, \qquad (2)$$

where $P(E) = \exp(-R/(v\tau\gamma))$ is the probability that the neutrons will survive the transit from the Sun to the Earth; $A(E)$ is the effective area of COMPTEL for neutron detection (Bhattacharya, D., private communication 1995, published by Nieminen 1997); $f(E)$ is the time integrated neutron emissivity at the Sun for the period from T_s =08:26 UT to T_f =09:25 UT in units of neutrons/(sr MeV); $T_0^*(E) = \max(T_0(E), T_s)$; $W(T_0^*(E), T_1(E))$ is the energy dependent normalization factor calculated using the microwave emission intensity-time profile. This normalization factor is defined by

$$W(T_0, T_1) = \int_{T_s}^{T_f} j_{mw}(t)\mathrm{d}t \Big/ \int_{T_0}^{T_1} j_{mw}(t)\mathrm{d}t. \qquad (3)$$

By averaging $f(E)$ over the energy bin i, we have

$$\langle f(E)\rangle_i = N_i R^2 \Big[\int_{E_i}^{E_{i+1}} \frac{A(E)P(E)}{W(T_0^*(E), T_1(E))}\mathrm{d}E\Big]^{-1}, \qquad (4)$$

and the mean emissivity in units of neutrons/(sr s MeV) at the Sun during the time interval for which both the COMPTEL neutron measurements and the microwave data are available, is given by $\varepsilon_i = \langle f(E)\rangle_i/(T_f - T_s)$. The obtained quantities of ε_i are shown in Fig. 2.

Several alternative analyses were carried out by Nieminen (1997). Neutron spectra were deconvolved using different microwave profiles from 8.4 GHz (Bern) to 15.4 GHz (Learmonth). Additionally an exponential time dependence with arbitrary decay time was analyzed by the maximum likelihood ratio method. It turns out that all deduced neutron spectra agree within statistical errors. The exponential time-decay constant from the maximum likelihood ratio method corresponds well to the average decay of the microwave emission. These results support the use of the microwave profile for the deconvolution.

We continue the present analysis with the spectrum of the primary ions producing the neutrons in nuclear interactions with solar matter. A power law spectrum of the interacting ions is employed, $N(E) \sim E^{-S}$, with cut-off energy ϵ. Thus we use for the analysis a solar neutron injection spectrum, $F_{\rm n}(E, S, \epsilon)$ (neutron/MeV), which is the spectrum of neutrons produced by ions with a power law spectrum in energy (the neutron spectrum itself is not a power law). The energy spectrum of neutrons produced by those ions in the solar atmosphere was calculated for the isotropic thick target model by means of the Monte Carlo technique (Hua & Lingenfelter 1987, Gueglenko et al. 1990). The $F_{\rm n}(E, S, \epsilon)$ spectrum is used as a theoretical tool for the analysis. Only a comparison of calculations with experimental data may reveal the most plausible approximations for the actual spectra of the interacting protons and the secondary neutrons. However, the convenience of $F_{\rm n}(E, S, \epsilon)$ is that it indicates the normalization and slope of the interacting proton spectrum in the corresponding energy band. The employed cut-off energy is very high, $\epsilon = 20$ GeV, so that even one order of magnitude lower value of ϵ would result in the same neutron spectrum in the COMPTEL energy range. Adopted ion abundances for the gradual phase of the flare correspond to Composition 1 of Ramaty et al. (1993). The best fit total number of > 30 MeV protons, $N_{\rm p}(> 30\ \mathrm{MeV})$, deduced for different proton spectral indexes, S, is shown in Fig. 3 as the median line of region a. The

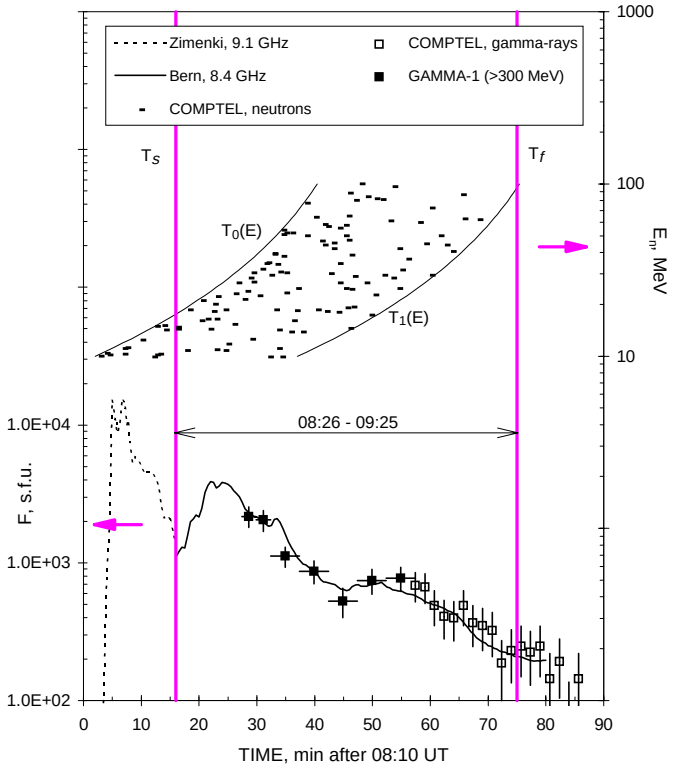

Fig. 1. COMPTEL neutron events corrected for the arrival time delay $\Delta T(E)$ (above) compared with the microwave and γ-ray emissions (below). We show the 9.1 GHz intensity-time profile for the impulsive phase and the 8.4 GHz profile for the gradual phase of the 15 June 1991 solar flare (curves). Also shown are the COMPTEL 0.8–30 MeV and GAMMA-1 > 300MeV γ-ray profiles (points, arbitrary intensity scale).

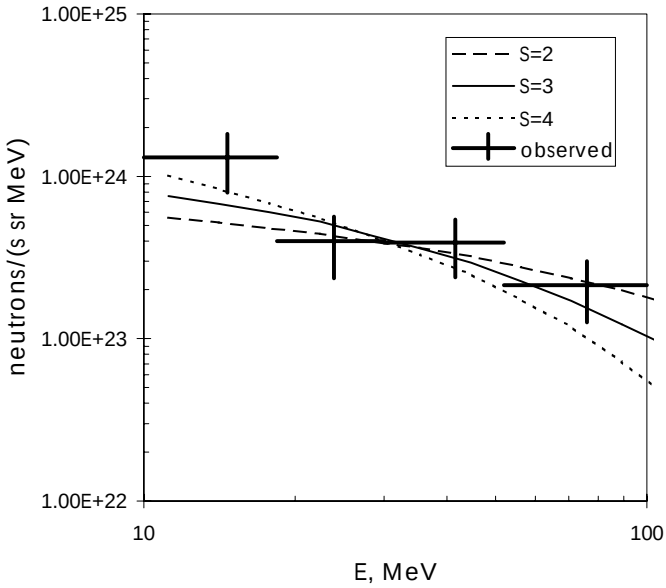

Fig. 2. Solar neutron emissivity corresponding to the electromagnetic emission arrival period 8:26–9:25 UT 15 June 1991. Points were deduced from the COMPTEL observations (Nieminen 1997). Curves were calculated proposing the interacting proton spectra to be a power law in energy with spectral index S. Curves were normalized to get the best fit to the observations (see the median line of the region a in Fig. 3).

region of possible values of $N_{\rm p}(> 30\ {\rm MeV})$ corresponding to the 70% confidence level is bounded by the thick solid line. It is seen that the COMPTEL neutron observations can be fitted with a rather wide variety of spectra corresponding to $S < 4.2$, because of the flattening of any secondary neutron spectra at low energies (Fig. 2).

To ascertain possible parameters of the interacting protons at the Sun, one can also employ low energy γ-ray line observations. The COMPTEL γ-ray data have been used to calculate the 2.22 MeV and 4–7 MeV γ-ray line fluences for the flare. To deduce a γ-ray line fluence, the instrument response matrix has to be separately determined for each flare using a Monte Carlo simulation code (Stacy et al. 1996). For the time interval 09:02–09:40 UT on 15 June 1991, the fluence of the 2.22 MeV γ-ray line emission is obtained as 5.35 ± 0.7 photons/cm^2. In the 4–7 MeV band, the γ-ray line fluence is 6.65 ± 0.75 photons/cm^2. These values of the 2.22 MeV and 4–7 MeV fluences are about one half of the values used in our previous analysis (Kocharov et al. 1994), but the fluence ratio is almost the same. The fluence decrease is mainly due to a more detailed code for the CGRO mass model employed for generation of the response matrix.

It has been pointed out that, during the gradual phase of the 15 June 1991 flare, the intensity-time profiles of both the COMPTEL and GAMMA-1 γ-ray observations followed the microwave emission profile remarkably well. For this reason, we normalized the COMPTEL γ-ray line fluences to the 08:26–09:25 UT time interval using Eq. 3 with T_0 =09:02 UT and T_1 =09:40 UT. The corresponding normalization factor is $W(T_0, T_1) = W_{\rm CGRO} = 7.3$. Then theoretical calculations of the γ-ray-line emission production by Ramaty et al. (1993) were used to deduce the 4–7 MeV γ-ray line fluences corresponding to different parameters of the interacting proton spectra, $N_{\rm p}(> 30\ {\rm MeV})$ and S. We show in Fig. 3 the parameter region b, where the theoretical 4–7 MeV γ-ray line fluence is equal to the observed one. The width of the region corresponds to the 1σ statistical uncertainties in the experimental data.

Another important piece of information on interacting proton spectra is the 2.22 MeV to 4–7 MeV fluence ratio. The observed ratio $F(2.22{\rm MeV})/F(4-7{\rm MeV})$ is 0.8 ± 0.15. According to calculations by Ramaty et al. (1993), this implies a proton spectral index of $S = 3.5 \pm 0.3$. The corresponding region is marked with c in Fig. 3. It is seen from Fig. 3, that all three requirement can be met only in a very limited parameter-region. Hence we conclude that the COMPTEL neutron and γ-ray line observations can be fitted with a power law index of the interacting protons of $S = 3.3 \pm 0.1$ and a total number of > 30 MeV protons of $N_{\rm p}(> 30\ {\rm MeV}) = (2.9 \pm 0.4) \times 10^{32}$ (for the time interval 08:26–09:25 UT). The deduced proton spectrum is valid in the 10–200 MeV energy band which is effective for the production of the neutron and γ-ray emissions observed with COMPTEL. To deduce the proton spectrum above 200 MeV,

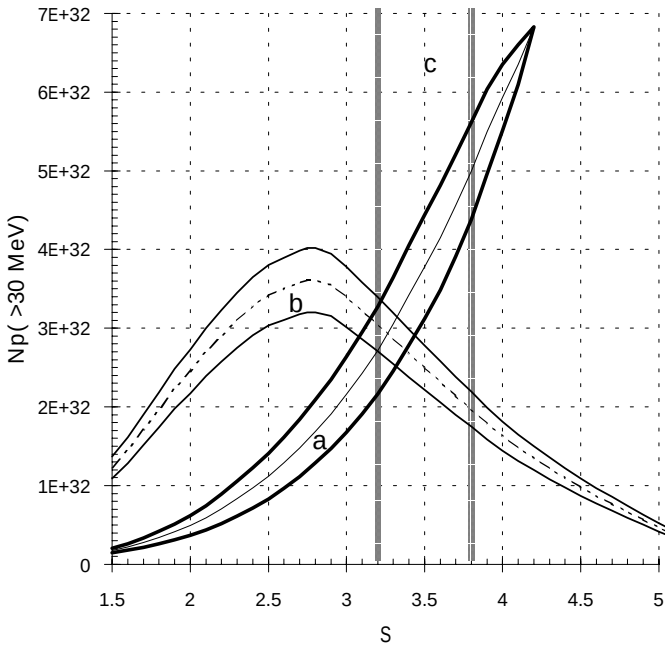

Fig. 3. Parameter space in the number of interacting protons, $N_{\rm p}(> 30\ {\rm MeV})$, and the proton spectral index, S. Method a uses 10–100 MeV neutron measurements, method b the fluence of the 4–7 MeV γ-rays and method c the 2.22 MeV to 4–7 MeV fluence ratio.

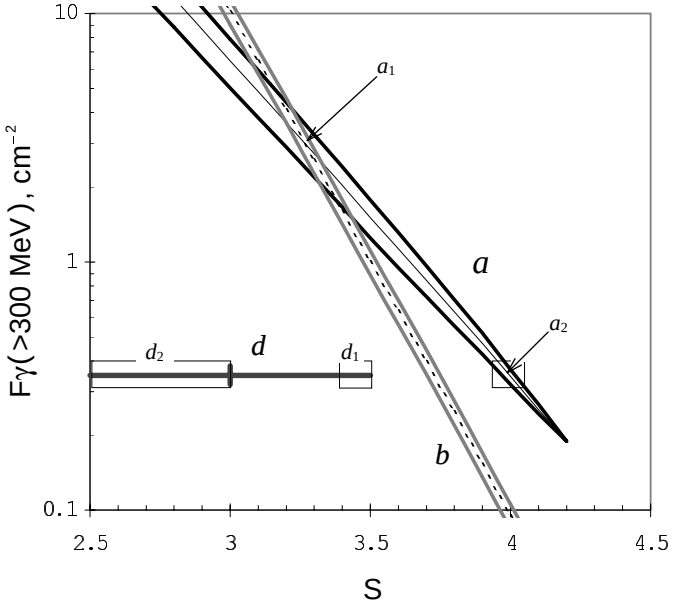

Fig. 4. The high-energy γ-ray fluences for the period 08:37–09:06 UT calculated for the power-law proton spectra with spectral indexes and normalizations being consistent with the low-energy COMPTEL measurements. The region a is deduced from the 10–100 MeV neutron observations, b is from the 4–7 MeV γ-ray line fluence. The median lines correspond to the best fits to the COMPTEL data. Parameters deduced from the GAMMA-1 measurements of the high-energy γ-ray emission are shown with the cross d. It is seen that the low-energy and high-energy observations can not be fitted by a single power law spectrum of interacting protons. Subregions a_1, a_2, d_1, and d_2 are used for the discussion.

observations of high-energy γ-ray emission should be additionally used.

3. High-energy γ-ray emission

Simultaneously with neutrons, π^0-mesons are produced which are the most likely source of the 100–2000 MeV γ-ray emission observed during the gradual phase of the 15 June 1991 flare on board the GAMMA-1 satellite (Akimov et al. 1991). It is possible that ultrarelativistic electrons and positrons also contribute the γ-ray emission at the low-energy end of the GAMMA-1 spectrum, $E_\gamma < 100$ MeV. For this reason, we deal in the present analysis especially with the high-energy portion of the spectrum, $E_\gamma > 100$ MeV. Furthermore, our principal conclusions are mainly based on the integral > 300 MeV γ-ray fluence, $F(> 300\ {\rm MeV})$, which is practically not sensitive to the deconvolution technique applied to the GAMMA-1 data. The fluence detected during 08:37–09:06 UT was $F(> 300\ {\rm MeV}) \approx 0.35\ {\rm cm}^{-2}$ (Chesnokov et al. 1995). On the other hand, given the spectrum of interacting protons, one can calculate the fluence of the pion-decay γ-ray emission. We assumed the same time-profiles for the production of the neutrons and pions (Lockwood et al. 1997) and used the thick target isotropic model of the π^0-meson production in the solar atmosphere (Gueglenko et al. 1990). We calculated the spectrum of the high-energy γ-ray emission originating from the decay of the π^0-mesons and compared it with the spectrum deconvolved by Djantemirov et al. (1995) using an updated response matrix of the GAMMA-1 instrument (see also Chesnokov et al. 1995).

As a first attempt, we assume that an unbroken power-law proton spectrum is valid up to 20 GeV. We show in Fig. 4 the calculated > 300 MeV γ-ray fluences corresponding to the proton power law spectra deduced from the COMPTEL observations. We employ both the spectral index, S, and the normalization, $N_{\rm p}(> 30\ {\rm MeV})$, required to fit the neutron and 4–7 MeV γ-ray line observations, i.e., the parameter regions shown in Fig. 4 map the parameter regions a and b of Fig. 3 onto the $F(> 300\ {\rm MeV}) - S$ plane. To calculate the > 300 MeV γ-ray fluence for the GAMMA-1 monitoring period, we again adopted the normalization factor defined by Eq. 3 with T_0 =08:37 UT and T_1 =09:06 UT: $W(T_0, T_1) = W_{\rm GAMMA1} = 2.2$. The cross d in Fig. 4 illustrates parameters deduced from the GAMMA-1 data (the rather large uncertainties in S are due to different deconvolution techniques applied; the midpoint corresponds to Kocharov et al. 1994, Chesnokov et al. 1995 and Djantemirov et al. 1995, the upper limit is given by results of Ramaty & Mandzhavidze 1994, the lower limit is the result of an another method of analysis, also considered by Chesnokov et al. 1995). It is seen that the case $S = 3.2 - 3.4$ and $N_{\rm p}(> 30\ {\rm MeV}) = (2.9 \pm 0.4) \times 10^{32}$, which fits the neutron and 4–7 MeV γ-ray line data, definitely overestimates the > 300 MeV γ-ray fluence. We also see that none of the unbroken power law spectra of interacting protons can fit all available data on the neutral emissions observed during the gradual phase of the

15 June 1991 solar flare. At low energies, the proton spectral index is deduced to be ≈ 3.3, but some steepening of the proton spectrum is needed above 200–300 MeV. Above ≈ 1 GeV, a new hardening of the proton spectrum is necessary to fit observations of the pion-decay emission at the high-energy end of the GAMMA-1 spectrum. Here, the power-law spectral index of the interacting protons was previously estimated in the thick target isotropic model as $S \approx 3$.

As a second attempt, we adopt the following spectrum of interacting protons:

$$N_{\rm p}(E) = A_1\Phi(E) + A_2E^{-S_3}, \quad (5)$$

where

$$\Phi(E) = \left(\frac{E}{E_0}\right)^{-S_1}\theta(E_0 - E) + \left(\frac{E}{E_0}\right)^{-S_2}\theta(E - E_0)\,, \quad (6)$$

$E_0 = 300\,\mathrm{MeV}$, $\theta(x) = 1$ for $x \geq 0$ and $\theta(x) = 0$ for $x < 0$. The normalization factor A_1, and spectral index S_1 are sampled at the intersection of the three regions shown in Fig. 3: $N_1(> 30\,\mathrm{MeV}) = 3.1 \times 10^{32}$, $S_1 = 3.3$. The normalization factor A_2 and the spectral index, $S_3 = 3$, were selected to fit the GAMMA-1 observations at the highest energies, $E_\gamma >$300 MeV. The normalization, A_2, corresponds to the number of > 30 MeV protons during the 08:26–09:25 UT interval, $N_2(> 30\,\mathrm{MeV}) = 1.1 \times 10^{31}$. The spectral index, S_2, has been adjusted to fit the > 100 MeV γ-ray spectrum. The final interacting-proton and secondary-photon spectra are shown in Fig. 5. Note the pronounced increase in the π^0-decay γ-ray emission below ≈ 300 MeV caused by a steepening of the proton spectrum to the left from the point 'C' in Fig. 5*b*. It is seen that the broken power law spectrum of the interacting protons naturally explains the observed > 100 MeV γ-ray spectrum. We conclude that the interacting proton spectrum as shown in Fig. 5*b* fits the 10–100 MeV neutron, the low-energy γ-ray line and the > 100 MeV γ-ray emissions observed during the gradual phase of the 15 June 1991 solar flare.

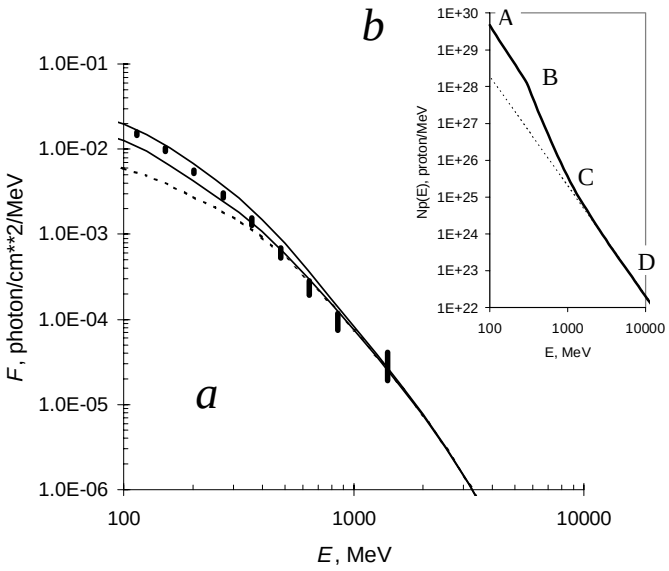

Fig. 5. Experimental (bars) and theoretical (curves) high-energy γ-ray spectra (panel *a*) and the interacting proton spectrum (panel *b*). The experimental points are from Chesnokov et al. (1995) (also Djantemirov et al. 1995). The proton spectrum is shown for $S_2 = 5.5$, the theoretical γ-ray spectra correspond to $S_2 = 5$ and $S_2 = 6$ (upper and lower solid curves, respectively); S_1=3.3; S_3=3. Dotted lines in both panels correspond to a single power law spectrum of inte racting protons with S=3.

4. Discussion

The time shifts in the COMPTEL γ-ray and neutron as well as in the GAMMA-1 monitoring periods complicate the analysis of the 15 June 1991 flare, as mentioned above. To solve the problem, a microwave intensity-time profile may be used (see Eq. 3). A comparison of the 15.4 GHz and 8.8 GHz intensity-time profiles (Nieminen 1997) revealed that, during the period 08:26–08:45 UT, their ratio tends to decrease from 0.96 to 0.75, and stayed nearly constant, ≈ 0.75, after 08:45 UT. Akimov et al. (1996) published results of the Bern microwave observations up to 50 GHz, which confirm that higher frequency emissions decayed slightly faster, and the microwave source became clearly optically thin at 8.4 GHz only after 08:45 UT. Consequently, the choice of the microwave frequency may slightly affect the normalization factors $W(T_0^*(E), T_1(E))$, $W_{\rm CGRO}$ and $W_{\rm GAMMA1}$. However, there are two different periods: (Period 1) 08:26–08:37 UT, where we have no γ-ray observations, and (Period 2) 08:37–09:25 UT, where the γ-ray intensity-time profile is available (Fig. 1). For the Period 2, we can verify microwave profiles against that of γ-rays and adopt only those microwave profiles which agree with the observed γ-ray profile. This limits a variance of acceptable microwave profiles, so that not more that $\approx 10\%$ error may come from the choice of the microwave frequency. During the Period 2, the 8.4 GHz profile fits well that of γ-rays (Fig. 1) and can be adopted as an approximation of the neutron production, because both neutrons and γ-rays are of the common proton origin. For the Period 1, we have to rely only on microwave time profile which may not exactly follow production of accelerated particles. Consequently, uncertainties during Period 1 are larger, but this period has almost no impact on positions of regions a, b and d shown in Fig. 4, because those regions are shown for the period of GAMMA-1 observations, 08:37–09:06 UT, which is completely inside the Period 2. If we employed a higher frequency emission, which actually decayed slightly faster than that of 8.4 GHz, the intersection of regions a and b in Fig. 4 (subregion a_1) would be positioned slightly higher, even farther from the region d, because a faster time decay results in higher values of all normalization factors and a higher value of the ratio $W_{\rm CGRO}/W_{\rm GAMMA1}$. Hence, our choice of the microwave frequency does not affect our principle conclusions drawn from Fig. 4. Only the total number of protons, $N_{\rm p}(> 30\,\mathrm{MeV})$ in Fig. 3, may be higher by about 20%.

The average slope of interacting proton spectrum between ≈ 100 MeV and ≈ 1300 MeV is not sensitive to the normalization procedure, because it depends on the relative number of 30–50 MeV neutrons and > 300 MeV photons, emissions generated at the Sun nearly simultaneously (Fig. 1). If we ignored the

COMPTEL γ-ray line and GAMMA-1 spectral information and employed only the neutron emissivity and the integral > 300 MeV γ-ray fluence, we would be able to accept a single power law spectrum of interacting protons with spectral index $S = 4 \pm 0.05$ (subregion a_2 in Fig. 4). From this, we can conclude that the proton spectral index in the region 'B–C' (Fig. 5*b*), $S_{\rm BC}$, is greater than 3.95, independently on the normalization procedure adopted. To the left from the point 'A', the deduced spectral index, $S_{\rm A} \approx 3.3$, depends on the adopted value of the normalization factor $W_{\rm CGRO}$. However, from the 2.22 MeV to 4 –7 MeV fluence ratio, which is normalization-independent, follows for the proton spectral index $S_{\rm A} < 3.8$ (Fig. 3). Hence, what ever the normalization may be, the spectral index changes at the point 'B' by $\Delta S_{\rm B} > 0.15$, and it is the most likely that $\Delta S_{\rm B} > 0.55$. At the highest energies, to the right of point 'C', the proton spectral index is normalization independent because it was deduced from the GAMMA-1 spectral data alone: $S_{\rm D} < 3.5$ and most likely $S_{\rm D} = 3$. In any case, the change in the proton spectral index at the point 'C' is necessary: $|\Delta S_{\rm C}| > 0.45$.

The COMPTEL instrument can measure γ-ray photons with energies from 0.8 to 30 MeV, while the GAMMA-1 range starts just at the photon energy of 30 MeV and extends up to ~ 10 GeV. Before the present analysis was started, we had used the microwave time profile to verify the consistency of GAMMA-1 and CGRO γ-ray spectra. Both γ-ray spectra were normalized using Eq. 3 and plotted together (see Rank et al., 1997). The CGRO spectrum near 30 MeV and different deconvolutions of the GAMMA- 1 spectrum, excluding only that of Akimov et al. (1996), agreed reasonably well. In this sense, employed data sets and the normalization method are selfconsistent.

Composition of interacting particles and especially $\alpha/{\rm p}$ ratio is an important parameter in the computation of the neutron production. We employ Composition 1, the photospheric composition with $\alpha/{\rm p} = 0.1$, as our basic for the analysis. While we do not consider ion abundances at the Sun as a free parameter, the parameter sensitivity should be estimated. Ramaty et al. (1993) along with Composition 1 also introduced Composition 2, in which accelerated particles are strongly enriched in helium ($\alpha/{\rm p} = 0.5$) and heavier elements. For instance, the accelerated Fe abundance relative to protons exceeds by more than order of magnitude the interplanetary observed value for impulsive solar flares, the photospheric Fe/p by almost a factor of 200, and that of the corona by 30. The suggested $\alpha/{\rm p}$ ratio corresponds to the upper limit for impulsive solar particle events observed at $\sim 1 - 10$ MeV/n (e.g., Kocharov and Kocharov, 1984) and exceeds by more than order of magnitude the ratio observed at $\sim 10 - 100$ MeV/n in the interplanetary medium during large solar particle events (e.g., Mazur et al., 1992). According to calculations by Ramaty et al. (1993), the choice of Composition 2 at spectral index $S = 3.3$ increases the neutron and 4–7 MeV γ-ray productions in respect to Composition 1 by factors $R_n \approx 4$ and $R_{4-7} \approx 6$, respectively, and fewer accelerated protons are correspondingly needed to produce the same amount of neutrons and γ-rays. However, the 2.22 MeV to 4.44 MeV fluence ratio is much less sensitive to the choice of composition.

If we employed Composition 2 instead of Composition 1, the spectral index S_1, being deduced from Fig. 3, would slightly decrease, by ~ 0.3, while the total number of protons, $N_{\rm p}(> 30\,{\rm MeV})$, would decrease by factor $\sim R_{4-7}$. Spectral index at highest energies, S_3, is almost independent on composition, because π^0-mesons are mainly produced in pp-reactions. However, the spectral index S_2, which depends on relative production of 10–100 MeV neutrons and pion-decay γ-rays, is rather sensitive function of composition. Production of 10–100 MeV neutrons depends on the composition of 20–200 MeV/n accelerated ions. In this energy range, helium-to-proton ratio may be less than the value of 0.1 suggested in Composition 1. In this case, the subregion a_1 in Fig. 4 moves upwards, farther from the region d, and spectral index S_2 (spectral steepening) increases. If the $\alpha/{\rm p} = 0.5$ is suggested (Composition 2), the subregion a_1 moves towards region d, and steepening decreases. However, even if we shifted the region a downwards by factor R_n and the region b by factor R_{4-7}, the subregion a_1 would be positioned still by factor 2–7 higher than the region d, and spectral steepening would still exist. Note that in the case of Composition 2 we even overestimated possible shift of the region a because (i) the factor R_n is energy integrated, while heavy elements contribute more in production of < 10 MeV neutrons not registered by COMPTEL, and (ii) helium still slightly contributes to the pion production. We can not rule out that the composition of interacting particles might be arbitrary adjusted to meet a single power law spectrum somewhere in the parameter region $\alpha/{\rm p} > 0.5$, but to the best of our knowledge, such values of $\alpha/{\rm p}$ in the 20–200 MeV/n energy range were never observed. We conclude that in our present understanding of solar particle abundances, it is unlikely that neutrons and γ-ray emissions detected during the gradual phase of the 15 June 1991 solar flare were produced by protons with a single power law spectrum in energy extending from below ~ 10 MeV to above ~ 10 GeV.

We propose a two component spectrum of the interacting protons (components A_1 and A_2 in Eq. 5) because a hard-steep-hard behavior of the spectrum is not expected in a single commonly accepted acceleration model. Two components of interacting protons were earlier suggested for this flare by Kocharov et al. (1994). Our present spectrum is qualitatively similar to that of Kocharov et al. (1994), but the total number of interacting protons is only about one half of the value deduced in our previous analysis, because of a decrease in the experimental values of the γ-ray fluences both at low (CGRO) and high (GAMMA-1) energies. The neutron observations of the 15 June 1991 flare were never employed before, and uncertainties in the γ-ray data allowed Ramaty & Mandzhavidze (1994) to find in the continuous acceleration case that, for almost any compositions from Composition 1 to Composition 2, the data can be fitted by assuming a single power law spectrum of the interacting protons with $S = 3.4 - 3.5$. Roughly speaking, such a fit is based on two points in the interacting proton spectrum: (i) the number of > 30 MeV protons, which controls the nuclear deexitation line fluence, and (ii) the number of > 700 MeV protons controlling the π^0-decay emission. To add a "third point" to this picture, we

use the 10–100 MeV neutrons also observed with COMPTEL. This neutron emission depends mainly on the number of ~ 150 MeV protons which was just a missed point required to get a curvature of the interacting proton spectrum in the logarithmic scale. It is also important that we use the revised γ-ray data. It finally turns out that the "third point" is clear off an unbroken power law spectrum of interacting protons which was accepted basing on the 4–7 MeV and > 300 MeV γ-ray data.

No one spectrum of interacting protons extends to infinity, and the exponential cut-off energy, E_C, may be introduced: $N_{\rm p}(E) = A_2 E^{-S_3} \exp(-E/E_C)$. There is a difference between the old and new versions of the GAMMA-1 spectral data sets at highest energies (Ozerov, 1998). The older version, employed by Mandzhavidze et al. (1993) and Ramaty & Mandzhavidze (1994), resulted in a steeper proton spectra, illustrated by subregion d_1 in Fig. 4, and the cut-off energy, $E_C = 2.7$ GeV, while the updated deconvolutions (Chesnokov et al. 1995, Djantemirov et al. 1995) lead to somewhat harder spectra (subregion d_2 in Fig. 4) and the cut-off energy $E_C > 10$ GeV. The cross d in Fig. 4 even overestimates present day uncertainties in the value of the spectral index because it also includes the older result by Ramaty & Mandzhavidze (1994). Note that the exponential cut-off might be also introduced for the first component (A_1 in Eq. 5) instead of the power law steepening with spectral index S_2. For this component, the exponential cut-off energy might be ≈ 400 MeV.

There was an interesting discussion going on about continuous acceleration versus impulsive acceleration plus trapping scenario. In particular, Rank et al. (1995) argued that the analysis of different energy bands in the COMPTEL range (4–7 MeV, 2.22 MeV, and 8–30 MeV) as well as a comparison of the COMPTEL and EGRET data (> 30 MeV) favour continuous acceleration over the trapping scenario. To finalize this discussion, Kovaltsov et al. (1995) used the Alma-Ata neutron monitor data for 15 June 1991 to estimate an upper limit of the high-energy solar neutron emission. They checked the assumption of a delta-like proton acceleration during the impulsive phase of the flare followed by trapping, and they concluded that such a scenario is inconsistent with the neutron monitor observations, while the continuous acceleration after the impulsive phase does not contradict to the observations.

On the other hand, the continuous acceleration seems inconsistent with transport of interacting protons in the magnetic loop with exceptionally quiet turbulent conditions (weak pitch angle scattering) suggested by Mandzhavidze et al. (1993). Note that the weak pitch angle scattering model results in the highest value of the spectral index, $S_3 = 3.8$. Later, Ramaty & Mandzhavidze (1994) considered model of saturated (moderate) pitch angle scattering in the loop with vertical magnetic field at footpoints and also the isotropic thick target model. Deduced spectral index, S_3, was between 3.4 and 3.5 depending on the model (d_1 in Fig. 4). Thus, the model dependent spectral shift between the two latter models is not large: $\delta S \leq 0.1$. This shift is caused by the energy-dependent anisotropy of the pion-decay γ-ray emission in the loop. The higher is the energy, the higher is the relative number of secondaries produced towards the Sun and the lower is that towards the Earth. The same is valid for neutrons. If we employed for neutron production the loop model with the moderate pitch angle scattering and vertical magnetic field at footpoints, we would deduce even higher number of interacting ~ 150 MeV protons, because the Earth-directed neutron production in this model is lower than the isotropic one (e.g., Gueglenko et al 1990). However, Kocharov et al. (1997) pointed out that realistic magnetic field tilt at the loop footpoints can affect angular distribution of secondary emissions, strongly limiting their anisotropy. Zirin & Wang (1993) studied the tilt of magnetic field lines in the active region NOAA 6659 and discovered very complex magnetic environment including among others, multiple channels of the horizontal magnetic field. It was conclude that almost all of the large flares in this region occur in highly convoluted magnetic fields. Such a complex variety of the magnetic tilts obviously makes secondary emissions close to those of the isotropic thick target model, excluding probably nearly upward emissions, and renders the model dependent spectral shift, δS, for the near-limb flare definitely less than 0.1. For this reason, we have selected for our present analysis the isotropic thick target model. Estimated inaccuracy of this model is less than inaccuracy in experimental data employed.

Two components of the interacting protons were also found in the 24 May 1990 solar flare mainly with analysis of high-energy neutron and neutron-decay proton data sets (Kocharov et al. 1996, Debrunner et al. 1997). One interacting proton component exhibited the spectral index $S_1 \approx 1.6$ below 300 MeV and steepened at higher energies with $S_2 \approx 4.6$. The energy spectrum of another component was consistent with a single power law, $S_3 \approx 3$, extending up to some GeVs. These two components however occurred not exactly simultaneously, but the $S_1 - S_2$ component exhibited a more prolonged decay than the S_3 one. Spectrum of the $S_1 - S_2$ component of interacting protons was found to be close to the spectrum of protons injected into the interplanetary medium during about one hour after the flare, but no counterpart of the "single power law", S_3, component was observed in the interplanetary medium. The interplanetary proton spectrum of the 15 June 1991 event demonstrates a steepening at some hundreds MeV (Kocharov et al. 1994) which is qualitatively similar to the deduced spectrum of the soft component of the protons interacting with solar matter during the gradual phase of the flare (A_1 in Eq. 5). Composition of the 15 June 1991 solar particle event in the interplanetary medium was that of a typical gradual event (Cliver 1996). Qualitative similarity of spectra and possible similarity of compositions leave room for a similar origin of selected components of interacting and interplanetary particles. Such a possibility seems reasonable for the acceleration at spatial scales of $\sim (0.3 - 1) R_\odot$ during $\sim 10 - 60$ min after the impulsive phase of the flare.

5. Conclusion

We have presented the new results of the neutron and γ-ray observations on board COMPTEL GRO during the gradual phase of the 15 June 1991 flare and the newly developed method for

their complex analysis. As a result of the analysis, we conclude the following:

1. A joint analysis of the COMPTEL nuclear γ-ray line and neutron observations indicates that the interacting proton spectrum between ≈ 10 and ≈ 200 MeV was rather hard: the deduced spectral index is $S_1 = 3.3 \pm 0.1$. This value of S_1 is deduced at $\alpha/\mathrm{p} = 0.1$, being only slightly dependent on the composition.
2. At $\alpha/\mathrm{p} \leq 0.5$, the deduced spectrum of interacting protons steepens above ~ 300 MeV. The steepening is less pronounced at $\alpha/\mathrm{p} = 0.5$ and more abrupt at $\alpha/\mathrm{p} = 0.1$.
3. The GAMMA-1 observations of the high-energy γ-ray emission suggest that another proton component also existed on 15 June 1991, with somewhat harder spectrum extending up to ≥ 10 GeV. According to previous studies, the spectrum of this component is consistent with a power law in energy with spectral index $S_3 = 3 \pm 0.5$, being almost independent on the composition.
4. The broken power law spectrum of interacting protons shown in Fig. 5*b* fits well all available data, the 10–100 MeV neutron and both > 100 MeV and low-energy γ-ray data, at $\alpha/\mathrm{p} = 0.1$.
5. A further search for a hypothetical single power law spectrum of interacting protons extending from some MeVs to above 10 GeV (e.g. Guglenko et al. 1990) might be possible when after a clear observational evidence has been delivered that the composition of high-energy solar particles interacting during gradual phase of the flare is enhanced in helium up to $\alpha/\mathrm{p} \sim 1$.

Acknowledgements. The COMPTEL project is supported by NASA under contract NAS5-26645, by the Deutsche Agentur für Raumfahrtangelegenheiten (DARA) under grant 50QV90968 and by the Netherlands Organization for Scientific Research (NWO). The study in Finland under the Cycle 5 CGRO Guest Investigator Program was supported by the Academy of Finland. G. K. was also supported by the grant RFFI 97-02-18073 and by the Nordic Council of Ministers under the CIMO research scholarship.

References

Akimov, V. V., Afanassyev, V. G., Belaousov, A. S., et al., 1991, Proc. 22nd Internat. Cosmic Ray Conf., Dublin, 3, 73
Akimov, V. V., Ambrož, P., Belov, A. V., et al., 1996, Solar Phys., 166, 107
Chesnokov, V. Yu., Djantemirov, H. M., Galper, A. M., et al., 1995, in: Biannual report '93, 94, ed. V. N. Nevolin, Moscow State Engineering Physics Institute Printing House, ISSN 0135-0966, p. 91
Cliver, E. W., 1996, in: High Energy Solar Physics, eds. R. Ramaty, N. Mandzhavidze, & X.-M. Hua, AIP Conf. Proc. 374, 45
Debrunner, H., Lockwood, J. A., Barat., C., et al., 1997, ApJ, 479, 997
Djantemirov, H. M., Galper, A. M., Khodarovich, A. M., et al., 1995, Proc. 24nd Internat. Cosmic Ray Conf., Rome, 4, 94
Gueglenko, V. G., Kocharov, G. E., Kovaltsov, G. A., et al., 1990, Solar Phys., 125, 91
Guglenko, V. G., Efimov, Yu. E., Kocharov, G. E., et al., 1990, ApJS, 73, 209
Hua, X.-M., & Lingenfelter, R. E., 1987, Solar Phys., 107, 351
Kahler, S., 1994, ApJ, 428, 837
Kane, S. R., Hurley, K., McTiernan, J. M., 1995, ApJ, 446, L47
Kocharov, L. G., & Kocharov, G. E., 1984, Space Sci. Rev., 38, 89
Kocharov, L. G., Kovaltsov, G. A., Kocharov, G. E., et al., 1994, Solar Phys., 150, 267
Kocharov, L. G., Torsti, J., Vainio, R., et al., 1996, Solar Phys., 169, 181
Kocharov, L. G., Torsti, J., Tang, F., et al., 1997, Solar Phys., 172, 271
Kovaltsov, G. A., Usoskin, I. G., Kocharov, L. G., et al., 1995, Solar Phys., 158, 395
Lockwood, J. A., Debrunner, H., Ryan, J. M., 1997, Solar Phys., 173, 151
Mandzhavidze, N., & Ramaty, R., 1993, Nuclear Phys. B, 33A,B, 141
Mandzhavidze, N., Ramaty, R., Akimov, V. V., Leikov, N. G., 1993, Proc. 23rd Internat. Cosmic Ray Conf., Calgary, 3, 119
Mazur, J. E., Mason, G. M., Klecker, B., McGuire, R. E., 1992, ApJ, 401, 398
McConnell, M, Bennett, K., Forrest, D., et al., 1993, Adv. Space Res., 13, (9)245
Nieminen, P., 1997, Neutrons from the 15 June 1991 Solar Flare, Dissertation, University of Bern
Ozerov, Yu. V., 1998, private communication
Ramaty, R., & Mandzhavidze, N, 1994, in: High Energy Solar Phenomena, eds. J. M. Ryan & W. T. Vestrand, AIP Conf. Proc. 294, 26
Ramaty, R., Mandzhavidze, N., Kozlovsky, B., et al., 1993, Adv. Space Res., 13, (9)275
Rank, G., Bennett, K., Bloemen, H., et al., 1995, in: High energy Solar Physics, eds. R. Ramaty, N. Mandzhavidze, X.-M. Hua, AIP Conf. Proc. 374, 219
Rank, G., Debrunner, H., Kocharov, L., et al., 1997, Proc. 25th Internat. Cosmic Ray Conf., Durban, 1, 1
Ryan, J., Bennett, K., Debrunner, H., et al., 1993, Adv. Space Res., 13, (9)255
Ryan, J. M., & McConnell, M. M., 1995, in: High energy Solar Physics, eds. R. Ramaty, N. Mandzhavidze, X.-M. Hua, AIP Conf. Proc. 374, 200
Schönfelder, V., Bennett, K., Bloemen, H., et al., 1993, ApJS, 86, 657
Stacy, J. G., Kippen, R. M., Kappadath, S. C., et al., 1996, A&AS, 120, 691
Trottet, G., Vilmer, N., Barat, C., et al., 1993, A&AS, 97, 337
Zirin, H., & Wang, H., 1993, Nature, 363, 426